European Journal of Neuroscience, Vol. 16, pp. 1647–1653, 2002

No evidence for calcium electrogenic exchanger in frog semicircular canal hair cells

M. Martini,[1] M. L. Rossi,[1] F. Farinelli,[1] A. Moriondo,[1] F. Mammano[2] and G. Rispoli[1]
[1]Dipartimento di Biologia, Sezione di Fisiologia e Biofisica, Istituto Nazionale di Fisica della Materia e Centro di Neuroscienze Università di Ferrara, via Borsari, 46, 44100 Ferrara, Italy
[2]Settore di Biofisica e Istituto Nazionale di Fisica della Materia, International School for Advanced Studies (SISSA), via Beirut 2–4, 34014 Trieste, and Venetian Institute of Molecular Medicine (VIMM), Università di Padova, via Orus 2, 35129 Padova, Italy

Keywords: Ca^{2+} imaging, caged compound photolysis, electrogenic pumps, frog labyrinth, gecko rods

Abstract

We investigated the possibility that, in hair cells mechanically isolated from frog semicircular canals, Ca^{2+} extrusion occurs *via* a $Na^+ : Ca^{2+}$ (cardiac type) or a $Na^+ : Ca^{2+},K^+$ (retinal type) exchanger. Cells concurrently imaged during whole-cell patch-clamp recordings using the Ca^{2+} sensitive fluorescent dye Oregon Green 488 BAPTA-1 (100 μM) showed no voltage dependence of Ca^{2+} clearance dynamics following a Ca^{2+} load through voltage-gated Ca^{2+} channels. Reverse exchange was probed in hair cells dialyzed with a Ca^{2+}- and K^+-free solution, containing a Na^+ concentration that saturates the exchanger, after zeroing the contribution to the whole-cell current from Ca^{2+} and K^+ conductances. In these conditions, no reverse exchange current was detected upon switching from a Ca^{2+}-free external solution to a solution containing concentrations of Ca^{2+} alone, or Ca^{2+} + K^+ that saturated the exchanger. By contrast, the same experimental protocol elicited peak exchange currents exceeding 100 pA in gecko rod photoreceptors, used as positive controls. In both cell types, we also probed the forward mode of the exchanger by rapidly increasing the intracellular Ca^{2+} concentration using flash photolysis of two novel caged Ca^{2+} complexes, calcium 2,2′-{[1-(2-nitrophenyl)ethane-1,2-diyl]bis(oxy)}bis(acetate) and calcium 2,2′-{[1-(4,5-dimethoxy-2-nitrophenyl)ethane-1,2-diyl]bis(oxy)}-bis(acetate), in the presence of internal K^+ and external Na^+. No currents were evoked by UV-triggered Ca^{2+} jumps in hair cells, whereas exchanger conformational currents up to 400 pA, followed by saturating forward exchange currents up to 40 pA, were recorded in rod photoreceptors subjected to the same experimental conditions. We conclude that no functional electrogenic exchanger is present in this hair cell population, which leaves the abundant plasma membrane Ca^{2+}-ATPases as the primary contributors to Ca^{2+} extrusion.

Introduction

Hair cells are compact sensory receptors endowed with synaptic function. Ca^{2+} ions play an essential role in hair cell functioning as localized changes of intracellular Ca^{2+} concentration ($[Ca^{2+}]_i$), both modulate the transduction process and regulate the amplitude of the cell receptor potential (reviewed in Fettiplace *et al*., 2001; Gillespie & Walker, 2001). The latter governs gating of Ca^{2+} and K^+ basolateral conductances, ultimately controlling transmitter release at the cell cytoneural junction (Lenzi & Roberts, 1994; Rossi *et al*., 1994; Fuchs, 1996). Thus, Ca^{2+} homeostasis in these cells is crucial for stimulus transduction and signal transmission to first-order neurons that relay sensory information to the central nervous system.

Given the relatively large Ca^{2+} influx through the voltage-gated basolateral Ca^{2+} channels in vertebrate hair cells, a mechanism of active Ca^{2+} transport across the membrane, that is a Ca^{2+}-ATPase and/or a Ca^{2+} exchanger, is expected to maintain Ca^{2+} homeostasis together with Ca^{2+} sequestration by intracellular buffers and organelles. In frog and guinea pig vestibular hair cells the presence of Ca^{2+} pumps at the level of the stereocilia, removing Ca^{2+} entering through the transduction channels, is well documented (Gioglio *et al*., 1998; Yamoah *et al*., 1998; Boyer *et al*., 2001; Dumont *et al*., 2001). Somewhat less clear-cut evidence supports the presence of mechanisms extruding Ca^{2+} across the synaptic pole plasma membrane. Ca^{2+} pumps have been found at the basal pole of turtle cochlear and frog saccular hair cells (Tucker & Fettiplace, 1995; Yamoah *et al*., 1998; Dumont *et al*., 2001). But a cardiac ($Na^+ : Ca^{2+}$) and a retinal-type ($Na^+ : Ca^{2+},K^+$) exchanger have also been described in guinea pig cochlear outer hair cells (Ikeda *et al*., 1992) and in guinea-pig type I vestibular hair cells (Chabbert *et al*., 1995; Boyer *et al*., 1999), respectively. This suggests that a Ca^{2+} exchanger might operate in frog vestibular hair cells as well. We therefore scrutinized the possible existence of a Ca^{2+} exchanger in our preparation using a combination of fast fluorescence Ca^{2+} imaging, patch-clamp recordings and UV flash photolysis of two novel Ca^{2+} cages. Results were compared to those obtained, under the same experimental conditions, from gecko rod photoreceptors, used as positive controls. Preliminary reports of this work have been presented in conference proceedings (Martini *et al*., 2002; Moriondo *et al*., 2002).

Materials and methods

Cell preparation and patch-clamp recordings

Hair cells were mechanically isolated from semicircular canals of the frog, *Rana esculenta* (Martini *et al*., 2000). Before dissection, the

Correspondence: Professor Giorgio Rispoli, as above.
E-mail: rsg@dns.unife.it

Received 17 April 2002, revised 27 July 2002, accepted 27 August 2002

doi:10.1046/j.1460-9568.2002.02234.x

frogs were anaesthetized by immersion in 1 g/L tricaine methanesulphonate solution and then decapitated. The head was pinned down at the bottom of the dissection chamber, and subsequently immersed in a dissection solution of the following composition (mM): 120 NaCl, 2.5 KCl, 0.5 ethylene glycol-bis(β-aminoethyl ether)*N*,*N*,*N*′,*N*′-tetracetic acid (EGTA), 5(*N*-2-hydroxyethylpiperazine-*N*′-(2-ethanesulphonic acid)) (Hepes), 20 sucrose, and 3 glucose (pH 7.2). The six ampullae were isolated from both labyrinths and transferred into the experimental chamber. The hair cells were mechanically dissociated from the ampullae by gently scraping the epithelium with fine forceps.

Rod outer segments (ROS) were mechanically isolated from the retina of the nocturnal lizard *Tokay Gecko* (Rispoli *et al*., 1995). All manipulations were made in the dark using infrared illumination and an infrared viewer (Find-R-Scope, FJW Optical Systems, Palatine, IL, USA). Before dissection, the geckos were dark adapted (≈4 h), anaesthetized with ether and then decapitated. Both eyes were removed from the head and hemisected. The back half of the eyeball was cut into four pieces that were stored in oxygenated Ringer solution on ice and used when needed. The composition of Ringer solution was (in mM): 160 NaCl, 3.3 KCl, 1 $CaCl_2$, 1.7 $MgSO_4$, 2.8 Hepes and 10 dextrose (pH 7.4). The retina was peeled from an eyecup piece and was gently stretched in ≈200 μL of Ringer to obtain the ROS; the fluid drop containing the ROS was then transferred to the recording chamber.

Cells were recorded using the whole-cell configuration of the patch-clamp technique under visual control at room temperature (20–22 °C) employing Axopatch 200B (Axon Instruments, Union City, CA, USA) or EPC-7 amplifiers (List-Electronic, Darmstadt, Germany). Data were acquired by a Digidata 1322A connected to the SCSI port of a Pentium computer running the pClamp 8.1 software package. When attempting to record reverse exchange currents, the external solution was rapidly exchanged by the horizontal displacement of a multibarrelled perfusion pipette placed in front of the recorded cell and driven by a computer-controlled stepping motor. Holding potentials (V_H) reported in this paper were corrected for the junction potential between the internal and the external solution, estimated using a dedicated routine of the Clampex 8.1 software package (Axon Instruments, Union City, CA, USA). The compositions of internal and external solutions differed for the various experimental protocols and are reported in the following subsections. The osmolality of all solutions was checked with a microosmometer (Hermann Roebling, Messtechnik, Berlin, Germany).

Ca^{2+} fluorescence imaging

Fluorescence imaging of $[Ca^{2+}]_i$ was performed as previously described (Mammano *et al*., 1999; Rispoli *et al*., 2001). Hair cells dissociated from the ampullae were plated under the microscope and continuously superfused with a Ringer solution containing 100 mM NaCl, 6 mM CsCl, 20 mM tetraethylammonium chloride (TEACl), 4 mM $CaCl_2$, 10 mM Hepes, and 6 mM glucose; pH 7.2. Cells were loaded through the patch pipette with the membrane impermeant form of the Ca^{2+}-selective dye Oregon Green 488 BAPTA-1 (OG) dissolved in the intracellular solution of the following composition: 92 mM CsCl, 20 mM TEACl, 2 mM $MgCl_2$, 1 mM ATP K^+ salt, 0.1 mM GTP Na^+ salt, 10 mM Hepes, 0.5 mM EGTA, and 0.1 mM OG; pH = 7.2. Fluorescence images were formed on a fast (15 MHz readout rate) and cooled CCD sensor (IA-D1; DALSA, Waterloo, Ontario, Canada); the sensor's output was digitized at 12 bit/pixel by customised electronics to produce 128 × 128 pixel images (resolution ≈0.5 μm/pixel) with an interframe interval of 4.1 ms (frame rate, 244 Hz). For each image pixel, fluorescence signals were computed as ratios: $\Delta F/F_o = [F(t) - F(0)]/F(0)$, where t is time, $F(t)$ is fluorescence following a voltage stimulus protocol that changes $[Ca^{2+}]_i$ within the cell and $F(0)$ is the prestimulus fluorescence (i.e. recorded at V_H) computed by averaging 10–20 images. Both $F(t)$ and $F(0)$ were corrected for mean background fluorescence; $\Delta F/F_o$ was smoothed with a two-dimensional 3 × 3 median filter and encoded by 8-bit look-up tables to produce 256 pseudo-colour indexed images.

Reverse mode exchange current recordings

To test for the presence and type of a functional electrogenic exchanger in hair cells, the experimental protocol described in Rispoli *et al*. (1995) was employed. Briefly, reverse exchange was probed in patch-clamped gecko ROS (positive controls) and frog hair cells dialysed with a Ca^{2+}- and K^+-free pipette solution containing a Na^+ concentration saturating the exchanger (in mM: hair cells, 100 NaCl, 20 CsCl, 5 TEACl, 0.5 $MgCl_2$, 1 ATP K^+ salt, 0.1 GTP Na^+ salt, 10 Hepes, and 2 EGTA; pH = 7.2. ROS, 166 NaCl, 10 Hepes, and 2 EGTA; pH = 7.2). The hair cell K^+ conductances were blocked by adding 15 mM TEACl and 5 mM CsCl to the external solution, and the Ca^{2+} currents were suppressed by 0.2 mM Cd^{2+} or by setting V_H to –70 mV. None of these conductances exists in the ROS, where the only membrane current pathways are the cGMP-gated channels and the $Na^+ : Ca^{2+},K^+$ exchanger (reviewed in Rispoli, 1998). The external perfusion solution was switched from a Ca^{2+}-free + xNa^+ solution (x = 115 mM in hair cells and 166 mM in ROS) to a solution containing 2 mM Ca^{2+}, expected to activate solely reverse $Na^+ : Ca^{2+}$ exchange. By contrast, switching to a 2-mM Ca^{2+} + 20 mM K^+ solution should activate both $Na^+ : Ca^{2+}$ and $Na^+ : Ca^{2+},K^+$ exchange. Ca^{2+} (and K^+, if the putative exchanger was of the retinal type) ions possibly accumulated during the reverse exchange operation would then activate forward exchange upon returning to the external Na^+ solution. The osmolality of the external perfusion solutions containing Ca^{2+} or Ca^{2+} + K^+ was kept at the control values (260 mOsm/kg in hair cells and 320 mOsm/kg in ROS) using either Li^+ or *N*-methyl-D-glucamine (NMG^+). No significant differences were found in the recordings from hair cells and ROS when using either cation type; the external solutions were buffered at the indicated pH values using 10 mM Hepes. To assess the actual amplitude of the reverse exchange current, i_{exch}, the raw data must be corrected for junction potential contribution as well as possible changes of leakage currents produced by different perfusion solutions. Accordingly, the following equation was used to derive i_{exch} from the raw data:

$$i_{exch} = i_a - i_b - \frac{V_H - V_J}{R_a} + \frac{V_H}{R_b} \quad (1)$$

where V_J is the junction potential between each solution pair (a and b), and R_a and R_b the respective cell input resistances.

Flash photolysis of caged compounds

Two novel caged Ca^{2+} complexes: calcium 2,2′-{[1-(2-*N*itrophenyl)-ethane-1,2-diyl]bis(oxy)}bis(acetate) and calcium 2,2′-{[1-(4,5-dimethoxy-2-nitrophenyl)ethane-1,2-diyl]bis(oxy)}bis(acetate), synthesized by Viappiani *et al*. (2002) and Rogolino *et al*. (Rogolino, D., Pelagatti, P., Carcelli, M. & Viappiani, C.; unpublished observation, 'Fast release of Ca^{2+} by a simple photosensitive chelator') were used to perform fast $[Ca^{2+}]_i$ changes. For the two photolabile chelators these authors have estimated the dissociation constants for Ca^{2+} both using potentiometric and spectroscopic methods based on the low

affinity fluorescent Ca^{2+} indicator Oregon Green 488 5 N at pH 7 in the presence of (in mM): 160 NaCl, 160 KCl, and 10 $MgCl_2$. The resulting dissociation constants were: 2.1 ± 0.1 μM for calcium 2,2′-{[1-(4,5-dimethoxy-2-nitrophenyl)ethane-1,2-diyl]bis(oxy)}bis-(acetate) and 2.6 ± 0.2 μM for calcium 2,2′-{[1-(2-nitrophenyl)-ethane-1,2-diyl]bis(oxy)}bis(acetate). Ca^{2+} complexes were stable upon increasing NaCl, KCl, and $MgCl_2$ up to (in mM): 200, 200, and 20, respectively. No evidence of ion replacement was found following Ca^{2+} increase in solution as shown by Oregon Green 488 5 N fluorescence emission, which remained unaffected by salt addition up to the above reported concentrations. The caged Ca^{2+} compounds were dissolved as 1 : 1 complexes, therefore the concentration of Ca^{2+} complexed to the ligands was the same as the concentration of the added caged compounds. The concentration of free Ca^{2+} in solution was determined by the dissociation constant: for example, a 4-mM caged Ca^{2+} solution had 90 μM free Ca^{2+}, in the absence of any other Ca^{2+} buffer. Recordings employing caged compounds were performed under dim ambient red lights. Cells on the microscope stage were illuminated with an ultrabright infrared LED (900 nm) and viewed on a TV monitor connected to a contrast enhancement camera (Till Photonics GmbH, Planegg, Germany) coupled to the microscope (TE 300, Nikon, Tokyo, Japan). To perform experiments on hair cells and ROS under the most similar conditions, both cell types were dialyzed with the same internal solution (in mM: 110 K-aspartate, 25 KCl, 10 NaCl, 5 Hepes, 6 $MgCl_2$, and 4 of each caged compound; pH 7.2) and bathed with a Ringer solution of the same composition (in mM: 137 NaCl, 1.7 $MgSO_4$, 1 $CaCl_2$, 5 dextrose, 6 glucose, 2.8 Hepes, 6 CsCl, and 20 TEACl; pH 7.2). Each caged compound was dissolved directly into the pipette solution and used immediately. UV flashes were delivered after approximately three minutes of whole-cell recording (to ensure cell loading with the caged compound) using a flash lamp coupled to the epifluorescence port of the microscope (FlashMic, Rapp OptoElectronic, Hamburg, Germany; flash duration and intensity: ≈5 ms and ≈0.05 mJ/flash, respectively). These compounds, as well as their uncaged form, resulted nontoxic to the cell at the concentrations employed here, as judged by unaltered cell morphology and stable electrophysiological recordings.

All compounds, except OG and Oregon Green 488 5 N (Molecular Probes, Eugene, OR, USA), and tricaine methanesulphonate (Sandoz, Basel, Switzerland), were purchased from Sigma (Sigma Chemical Co., St. Louis, MO, USA).

Values in the text are given as mean ± SEM.

Results

Response of isolated hair cells to voltage controlled Ca^{2+} loads

In hair cells of the frog semicircular canal Ca^{2+} current flows through L- and R-type Ca^{2+} channels, as previously described (Martini *et al*., 2000). During whole-cell recordings in which the Ca^{2+} fluorescent dye OG was used to monitor ion concentration changes, voltage-gated Ca^{2+} entry was found to occur at selected sites (hotspots) located around the cell synaptic pole (Rispoli *et al*., 2001).

Figure 1 shows an example of fluorescence response, obtained from a hair cell in the present series of experiments, following a 160-ms voltage command to –20 mV. The height of the 3D diagram gives fluorescence intensity along a medial line through the cell body (receding axis) vs. time (abscissa). During the presentation of the stimulus, fluorescence peaked characteristically near the cell base, where the Ca^{2+} channels are clustered, thereafter spreading throughout the cell body, as a consequence of diffusion, and declining due to Ca^{2+} removal following buffering and extrusion. To assess whether an exchanger mediated the Ca^{2+} extrusion phase, Ca^{2+} clearance dynamics was further investigated.

Insensitivity of hair cell Ca^{2+} concentration to after-stimulus potential changes

The rate of Ca^{2+} extrusion by any exchanger working in the forward mode is accelerated by hyperpolarization (reviewed in Blaustein & Lederer, 1999). Thus, in principle, returning the cell membrane potential to different after-stimulus values was expected to alter both tail currents and Ca^{2+} clearance dynamics.

This possibility was tested by stimulating the same cell twice with a 160-ms test depolarization to –20 mV from V_H = –70 mV and returning the membrane potential to an after-stimulus value of either –60 mV or –120 mV (Fig. 2A). The time-course of $[Ca^{2+}]_i$ changes were estimated by measuring the time-dependent fluorescence (monitored concurrently to the Ca^{2+} current) averaged in an 8 × 8-pixel region of interest (corresponding to an area of 4 μm^2 in the specimen plane) superimposed over a hotspot. During the test depolarization, fluorescence increased with no detectable lag from the onset of the Ca^{2+} current, as previously found, and started to decay immediately after stimulus offset, when the Ca^{2+} current began its rapid return to the prestimulus (zero) level (see also Rispoli *et al*., 2001). A pool of n = 5 cells, in which a total of 13 hotspots were counted, were selected for having a stable Ca^{2+} current amplitude throughout the recording. In these cells, fluorescence decayed at stimulus offset with a bi-exponential time-course as determined by nonlinear Levenberg–Marquardt fitting procedures. The decay time-course was negligibly affected by the after stimulus potential (time constants: τ_{11} = 130 ± 41 ms and τ_{21} = 2300 ± 800 ms at –60 mV; τ_{12} = 160 ± 30 ms and τ_{22} = 2500 ± 700 ms at –120 mV; Fig. 2A). The differences between time constants at these two voltages were not statistically significant (paired t-test). A similar experiment was performed on different cells, in which the after-stimulus potential was stepped from –60 to –120 mV during the same recording (Fig. 2B). Consistently with the above results, no changes in the time-course of fluorescence signal were detected during the after-stimulus potential change (n = 4), within the sensitivity limits of our technique. An estimate of this sensitivity was derived in a separate set of experiments, where changes in fluorescence amplitude and recovery time-course at selected hotspots were detected in response to changes of Ca^{2+} loads as small as 10% (n = 17; see also Fig. 4 of Rispoli *et al*., 2001). In summary, the results exemplified in Fig. 2 tended to rule out any significant contributions to Ca^{2+} homeostasis by an electrogenic exchanger. To substantiate this conclusion, we attempted to record exchange currents under conditions designed to maximize their amplitude, while excluding all other current sources.

Comparison of whole-cell current recordings from hair cells and ROS under conditions expected to activate Ca^{2+} exchangers

Exchange current activation was probed in patch-clamped gecko ROS (used as positive controls) and frog hair cells using the solution substitution protocol described in the Methods. As shown in Fig. 3A (left), peak exchange currents, flowing in the outward direction and occasionally exceeding 100 pA, were recorded in ROS bathed in the Ca^{2+} + K^+ test solution (average peak current: 66 ± 9 pA, n = 23). Ca^{2+} and K^+ ions, accumulated in the cell cytosol after a few minutes of reverse exchange activation, were enough to activate a nearly saturating forward exchange (inward) current upon returning the ROS

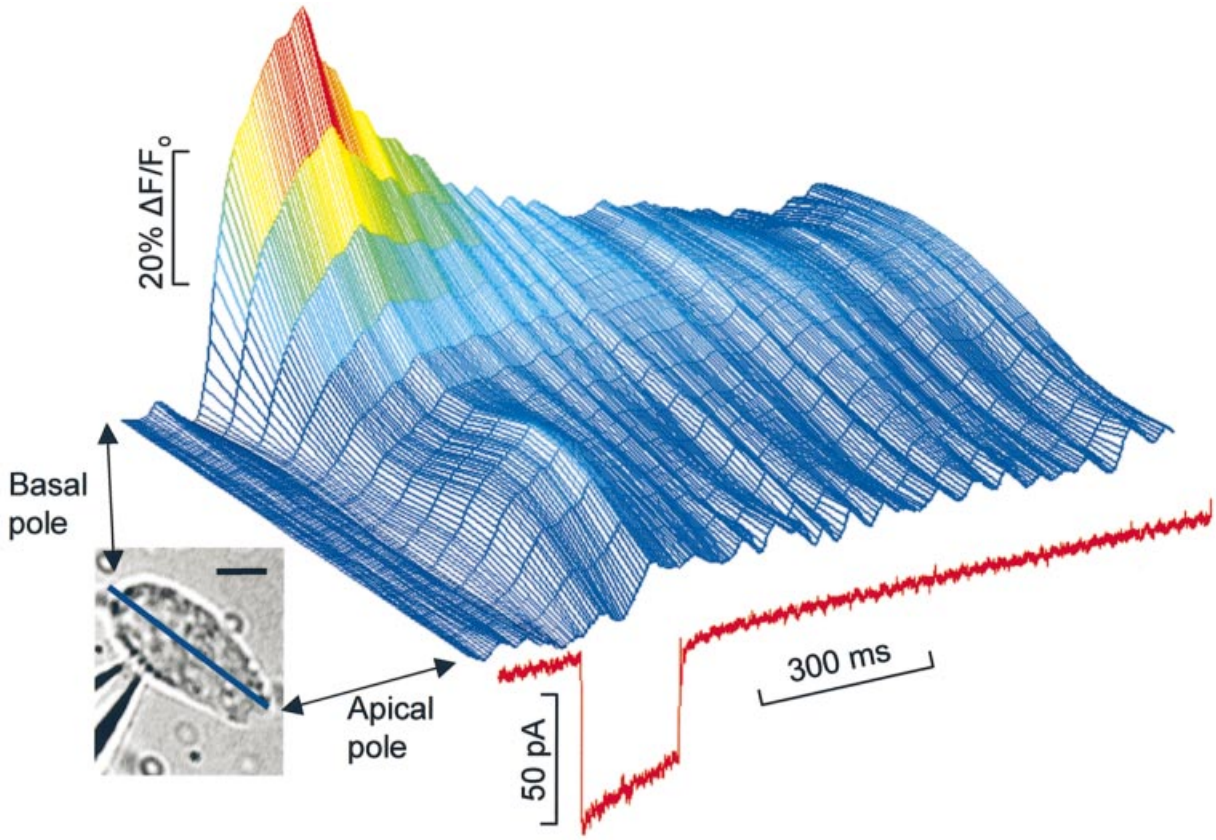

FIG. 1. Spatio-temporal Ca^{2+} dynamics in an isolated hair cell. Digital micrograph of the hair cell in bright field and space-time plot of the OG fluorescence; the cell was loaded with 0.1 mM OG through the patch pipette sealed to its base (see Methods). The spatial and temporal fluorescence changes, evoked by a 160-ms depolarization to –20 mV from a V_H of –70 mV, was measured along a 20-μm line (in blue) superimposed on the cell medial axis shown in bright field image (scale bar, in black, 5 μm). Abscissa is time; surface height and colour give local fluorescence change. The simultaneous leak-subtracted whole-cell current record is shown alongside the surface plot.

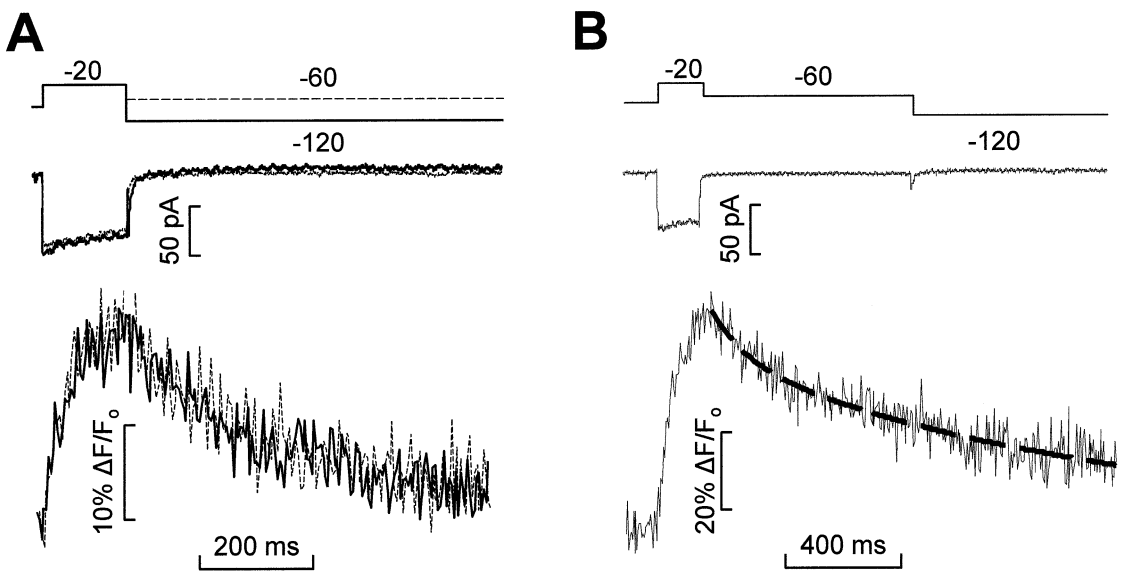

FIG. 2. Voltage independence of Ca^{2+} clearance dynamics in hair cells. (A) The same cell was stimulated twice by a 160-ms depolarization to –20 mV from a V_H of –70 mV. Dashed and continuous traces were obtained upon returning to an after-stimulus potential of either –60 or –120 mV (top panel); note nearly identical time-course of leak subtracted whole-cell currents (middle) and Ca^{2+}-induced OG fluorescence (bottom). (B) Similar experiment performed on a different cell, in which the after-stimulus potential was stepped from –60 to –120 mV during the recording; the thick dashed trace superimposed on the fluorescence record is a double exponential least square fit with time constants τ_1 = 0.125 s and τ_2 = 1.45 s. Note different time scale in A and B. In both cases, fluorescence was measured within an 8 × 8-pixel region of interest (corresponding to an area of 4 μm^2 in the specimen plane) superimposed over the brightest hotspot located at the cell basal pole.

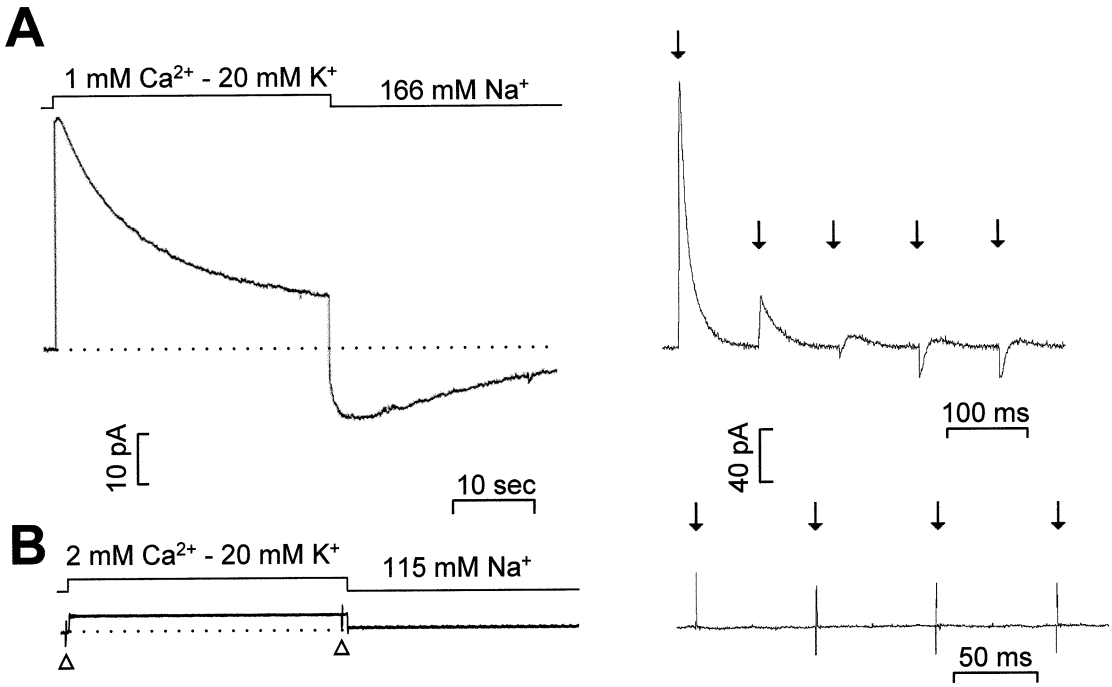

FIG. 3. Probing forward and reverse mode of the Ca^{2+} exchanger. (A) Left, whole-cell current recorded from a ROS while switching from a Ca^{2+}-free Na^+ external solution (containing 2 mM EGTA) to a solution containing 20 mM K^+, 1 mM Ca^{2+} and 145 mM Li^+; V_H = 0 mV; dotted line indicate 0 current. Right, stimulating the forward mode of exchange by application of a train of five UV flashes (downward arrows) to liberate a caged-Ca^{2+} compound dissolved in the patch pipette solution at 4 mM concentration; V_H = –30 mV. (B) Same as A, for a canal hair cell patched with similar pipette and external solutions (see Methods); left, 0.2 mM Cd^{2+} were present in the external solution (besides TEACl and CsCl) to block voltage-gated Ca^{2+} channels; V_H = 0 mV; –10 mV pulses (empty triangles) were delivered to test cell input resistance in Na^+ and in Ca^{2+} + K^+ perfusion solutions (≈4 GΩ in both solutions); right, the train of UV flashes elicited only brief electrical artifacts; V_H = –70 mV.

to the control Na^+ solution. The same experimental strategy was applied to all hair cell experiments.

In a group of 12 hair cells, the holding potential was set at V_H = –70 mV to prevent the opening of the voltage-dependent Ca^{2+} channels. In this group, input resistance was tested by applying a 10-mV hyperpolarization pulse from V_H (10 ms pulse duration). Na^+ was the major cation present in the control solution whereas the test solution contained either NMG^+ (n = 5) or Li^+ (n = 7). Two test solutions were employed to probe the exchange current (see Methods for detail of solution composition): one contained 2 mM Ca^{2+} alone (n = 8), whereas the other contained 2 mM Ca^{2+} + 20 mM K^+ (n = 4). In these experiments switching from control to test solution evoked a current change, whose amplitude remained constant throughout the application of the test solution (up to 30 s). This current was not generated by electrogenic transport, as it can be accounted for by the junction potential (V_J) between the adjacent perfusion solutions and by the difference in cell input resistance found in control (4.5 ± 1.1 GΩ; n = 12) and test solutions (7.7 ± 1.8 GΩ; n = 12). Indeed, applying Equ. 1 and correcting for $V_J(NMG^+)$ ≈3.2 mV and $V_J(Li^+)$ ≈0, the average current change evoked by the test solution turned out to be negligible (–0.7 ± 4.4 pA; n = 12).

As depolarization is expected to boost reverse exchange, a second set of 9 cells was tested at V_H = 0 mV. To block the voltage-gated Ca^{2+} channels, 0.2 mM Cd^{2+} was added to both control and test solutions. To keep V_j ≈0, Li^+ was selected as the major cation in both control and test solutions (the latter contained, as above, either 2 mM Ca^{2+} or 2 mM Ca^{2+} + 20 mM K^+). Again, after correcting for the cell input resistance change, no current was recorded in either one of the test solutions (Fig. 3B, left). Note that applying external Ca^{2+} at a concentration of 0.1 mM sufficed to activate saturating reverse exchange in ROS (data not shown). Instead, no sign of reverse exchange activation was detected in hair cells exposed to external Ca^{2+} concentrations as high as 2 mM (see for example Fig. 3B, left).

The negative result illustrated in Fig. 3B might be due, in principle, to unexpected (and unexplained) lack of reverse exchange activation under the above conditions. A further and direct test for forward exchange consists of dialyzing the cell with a solution containing high Ca^{2+} levels (and K^+, in the case of the retinal exchanger) while bathing it in a high Na^+ solution. When performing this experiment on ROS, a saturating forward exchange current was recorded using 20 mM Ca^{2+} in the patch pipette solution. Currents were up to 30 pA in the presence of external 160 mM Na^+ + 1 mM Ca^{2+} at V_H = –30 mV and approximately 1.6 ± 0.2-fold larger at V_H = –70 mV (n = 5, data not shown; see also Rispoli *et al*., 1996). Note that the $[Ca^{2+}]_i$ necessary to saturate the exchanger is approximately 50 μM, given an exchanger-Ca^{2+} dissociation constant of approximately 1 μM (Perry & McNaughton, 1993). The high Ca^{2+} concentration in the pipette solution reported above was required to compensate for buffered Ca^{2+} diffusion through the rod disk stack and steady state Ca^{2+} extrusion by the exchanger. By contrast, hair cells dialyzed with a pipette solution containing 3 mM Ca^{2+} gave no measurable exchange current at –70 mV (n = 3). Differently from ROS, Ca^{2+} concentrations larger than 3 mM in the pipette caused hair cell death, possibly due to activation of Ca^{2+}-dependent proteases (data not shown; see Martini *et al*., 2000). To avoid cell death whilst ensuring the possibility of achieving (at least transiently) Ca^{2+} concentrations at the intracellular aspect of the plasma membrane

capable of saturating the exchanger, we produced brief Ca^{2+} jumps by the UV flash photolysis of two novel Ca^{2+} caged compounds described in the Methods (Fig. 3, right panels). In a typical experiment, cells were dialyzed with a solution containing 135 mM K^+ and 4 mM of a Ca^{2+} cage (presaturated with Ca^{2+}). As shown in Fig. 3A (right), a progressive photo-induced cytosolic Ca^{2+} rise, promoted in ROS by a train of UV flashes delivered every 100 ms, evoked a transient outward current whose peak amplitude (initially very large: 260 ± 40 pA in response to the first flash; $n = 6$) progressively decreased, turning inward by the third flash (peak amplitude of the inward transient after the fourth flash: 30 ± 5 pA; $n = 6$). The working hypothesis to explain this phenomenology (Moriondo *et al*., 2002) resembles the one formulated by Kappl *et al*. (2001) for the cardiac exchanger. In brief, the simultaneous presence of external Na^+ and internal K^+ is thought to recruit a retinal exchanger state which produces an electrogenic conformational current in response to a $[Ca^{2+}]_i$ jump, generating the outward transient. This event precedes the onset of a full exchange cycle, which is initiated when $[Ca^{2+}]_i$ reaches a threshold level; for larger $[Ca^{2+}]_i$-values, a sustained inward current develops.

In hair cells ($n = 7$), besides brief electrical artifacts produced by the flash lamp, no current was elicited by the photolysis of either compound at $V_H = -70$ mV, even when the interflash period was decreased to 75 ms (Fig. 3B, right). In cells whose Ca^{2+} current either ran down or was blocked by external Cd^{2+} ($n = 4$), the $[Ca^{2+}]_i$ jump was also applied at $V_H = -20$ mV or +40 mV to maximize the putative outer conformational current and/or the inner exchange current. The recordings obtained under these conditions were similar to the one illustrated in Fig. 3B and therefore are not shown.

Discussion

The precise identity of the Ca^{2+} clearance mechanism across the plasma membrane is still controversial. It has been proposed that, in turtle cochlear hair cells, Ca^{2+} is cleared from its entry sites (clustered in hotspots) by basolateral Ca^{2+}-ATPases rather than a Ca^{2+} exchanger, besides being sequestered in the cisternae lining the cell lateral membrane (Tucker & Fettiplace, 1995). In frog canal hair cells, lead acetate precipitation experiments indicated that Ca^{2+}-ATPases are mainly located in the hair bundle, although limited staining of the cell basolateral membrane was also detected (Gioglio *et al*., 1998). However, this technique is less sensitive and specific than antibody staining, so the possible contribution of basolateral Ca^{2+}-ATPases might have been underestimated. Indeed, in the frog saccular hair cells, Yamoah *et al*. (1998), found intense labelling of the hair bundles and a fainter labelling of the basolateral membrane, using confocal immunofluorescence microscopy with monoclonal antibodies against plasma membrane Ca^{2+}-ATPases. Moreover, by screening saccular cDNA library and using immunocytochemistry and immunoprecipitation experiments, Dumont *et al*. (2001) demonstrated that the hair bundle possess an isoform of Ca^{2+}-ATPase different from the one in the basolateral membrane. Finally, in guinea pig vestibular hair cells, a central role of ciliary Ca^{2+}-ATPases was claimed by Boyer *et al*. (2001). According to these authors, such ATPases would remove Ca^{2+} entering the cell both through the transduction channels and through a novel L-type Ca^{2+} channels, located in the kinocilium. However, the presence of a Ca^{2+} exchanger is not definitely ruled out by the aforementioned results. Some reports even argue for the existence of a retinal type and a cardiac type exchanger in hair cells (Ikeda *et al*., 1992; Chabbert *et al*., 1995; Boyer *et al*., 1999).

In isolated guinea pig ventricular myocites, a slow negative tail current following a depolarizing stimulus is believed to reflect Ca^{2+} extrusion by $Na^+ : Ca^{2+}$ exchange (see, e.g. Fig. 4 in Hao *et al*., 1994). Despite displaying a similar time-course, the small negative tail of the whole-cell current recorded in hair cells, under comparable voltage protocols, reflects instead the slow deactivation of R-type channels. This was demonstrated in experiments where, before and after blocking the L-type component by nifedipine (see, e.g. Fig. 4 in Martini *et al*., 2000 and Fig. 5 in Rispoli *et al*., 2001), superimposable tail currents were recorded, despite the large difference of Ca^{2+} loads (up to 70%). Examining the recordings obtained during run-up of L-type Ca^{2+} current leads to a similar conclusion as, also in this case, tail currents obtained during the progressive increase (up to 50%) of the Ca^{2+} load (see, e.g. Fig. 11A and B in Martini *et al*., 2000 and Fig. 4 in Rispoli *et al*., 2001) were virtually indistinguishable from controls.

Furthermore, hyperpolarization did not modify Ca^{2+} clearance kinetics in any of the hotspots detected in the three hair cell types found in the *crista ampullaris*. Finally, no current was detected at different V_H (from –70 to +40 mV) when the forward or the reverse modes were tested, in the presence or in the absence of K^+ at the membrane side where Ca^{2+} was present. Altogether, the results presented in this paper lead us to exclude the involvement of any sort of Ca^{2+} exchanger in the homeostasis of $[Ca^{2+}]_i$ in frog canal hair cells.

Our diffusion kinetic studies showed that, upon entering the cell through voltage-gated channels, Ca^{2+} proceeds evenly towards the cell interior with an apparent diffusion constant of approximately 57 $\mu m^2/s$ (Rispoli *et al*., 2001). In the presence of effective extrusion and storage systems at the cell basolateral membrane, a different diffusion pattern would be expected, namely one whereby Ca^{2+} remains substantially confined in the neighbourhood of the entry sites. Nevertheless, we cannot exclude that a fraction of Ca^{2+} entering through voltage-gated Ca^{2+} channels is extruded by basolateral membrane Ca^{2+}-ATPases. If present, these pumps are unlikely to be electrogenic, otherwise their turnover rate would be voltage-sensitive (Hao *et al*., 1994), whereas we found that the Ca^{2+} clearance time-course was negligibly affected by the voltage (Fig. 2; see also Eisenrauch & Bamberg, 1990; Tucker & Fettiplace, 1995).

Irrespective of Ca^{2+}-ATPases location and mode of operation, our experimental results, ruling out the activity of any electrogenic exchanger, indicate that Ca^{2+}-ATPases represent the main route of Ca^{2+} removal. As Ca^{2+} entering the synaptic pole can be effectively shuttled by mobile buffers to the cell apex (Yamoah *et al*., 1998), the functional implication of our experiments is that the $[Ca^{2+}]_i$ rise at the cell base serves both as a proximal determinant for synaptic transmission and as a distant negative feedback signal for the transduction apparatus.

Acknowledgements

This work was supported by grants from the Istituto Nazionale per la Fisica della Materia (INFM), Line TS-B2 (F.M.) and Line FE-B2 (G.R.), the Ministero per l'Istruzione, l'Università e la Ricerca Scientifica (Cofin MIUR) to F.M. and M.L.R., and from Università di Ferrara (grant ex-60%) to G.R.

Abbreviations

$[Ca^{2+}]_i$, intracellular Ca^{2+} concentration; ROS, rod outer segment; OG, Oregon Green 488 BAPTA-1; V_H, holding potential.

References

Blaustein, M.P. & Lederer, W.J. (1999) Sodium/calcium exchange: its physiological implications. *Physiol. Rev.*, **79**, 763–854.

Boyer, C., Art, J.J., Dechesne, C.J., Lehouelleur, J., Vautrin, J. & Sans, A. (2001) Contribution of the plasmalemma to Ca^{2+} homeostasis in hair cells. *J. Neurosci.*, **21**, 2640–2650.

Boyer, C., Sans, A., Vautrin, J., Chabbert, C. & Lehouelleur, J. (1999) K^+-dependence of Na^+-Ca^{2+} exchange in type I vestibular sensory cell of guinea-pig. *Eur. J. Neurosci.*, **11**, 1955–1959.

Chabbert, C., Canitrot, Y., Sans, A. & Lehouelleur, J. (1995) Calcium homeostasis in guinea pig type-I vestibular hair cell: possible involvement of a Na^+-Ca^{2+} exchanger. *Hear. Res.*, **89**, 101–108.

Dumont, R.A., Lins, U., Filoteo, A.G., Penniston, J.T., Kachar, B. & Gillespie, P.G. (2001) Plasma membrane Ca^{2+}-ATPase isoform 2a is the PMCA of hair bundles. *J. Neurosci.*, **21**, 5066–5078.

Eisenrauch, A. & Bamberg, E. (1990) Voltage-dependent pump currents of the sarcoplasmic reticulum Ca^{2+}-ATPase in planar lipid membranes. *FEBS Lett.*, **268**, 152–156.

Fettiplace, R., Ricci, A.J. & Hackney, C.M. (2001) Clues to the cochlear amplifier from the turtle ear. *Trends Neurosci.*, **24**, 169–175.

Fuchs, P.A. (1996) Synaptic transmission at vertebrate hair cells. *Curr. Opin. Neurobiol.*, **6**, 514–519.

Gillespie, P.G. & Walker, R.G. (2001) Molecular basis of mechanosensory transduction. *Nature*, **413**, 194–202.

Gioglio, L., Russo, G., Marcotti, W. & Prigioni, I. (1998) Localization of Ca-ATPase in frog crista ampullaris. *Neuroreport*, **9**, 1309–1312.

Hao, L., Rigaud, J.L. & Inesi, G. (1994) Ca^{2+}/H^+ countertransport and electrogenicity in proteoliposomes containing erythrocyte plasma membrane Ca-ATPase and exogenous lipids. *J. Biol. Chem.*, **269**, 14268–14275.

Ikeda, K., Saito, Y., Nishiyama, A. & Takasaka, T. (1992) Na^+-Ca^{2+} exchange in the isolated cochlear outer hair cells of the guinea-pig studied by fluorescence image microscopy. *Pflügers. Arch.*, **420**, 493–499.

Kappl, M., Nagel, G. & Hartung, K. (2001) Voltage and Ca^{2+} dependence of pre-steady-state currents of the Na-Ca exchanger generated by Ca^{2+} concentration jumps. *Biophys. J.*, **81**, 2628–2638.

Lenzi, D. & Roberts, W.M. (1994) Calcium signaling in hair cells: multiple roles in a compact cell. *Curr. Opin. Neurobiol.*, **4**, 496–502.

Mammano, F., Canepari, M., Capello, G., Ijaduola, R.B., Cunei, A., Ying, L., Fratnik, F. & Colavita, A. (1999) An optical recording system based on a fast CCD sensor for biological imaging. *Cell Calcium*, **25**, 115–123.

Martini, M., Rossi, M.L., Farinelli, F. & Rispoli, G. (2002) Neither Na: Ca nor Na: Ca,K electrogenic exchanger exists in frog semicircular canal hair cells. *Biophys. J.*, **82**, 566a.

Martini, M., Rossi, M.L., Rubbini, G. & Rispoli, G. (2000) Calcium currents in hair cells isolated from semicircular canals of the frog. *Biophys. J.*, **78**, 1240–1254.

Moriondo, A., Rogolino, D. & Rispoli, G. (2002) Conformational changes of retinal exchanger probed with flash photolysis of novel Ca-caged compounds. *Biophys. J.*, **82**, 566a.

Perry, R.J. & McNaughton, P.A. (1993) The mechanism of ion transport by the Na^+: Ca^{2+}, K^+ exchange in rods isolated from the salamander retina. *J. Physiol. (Lond.)*, **466**, 443–480.

Rispoli, G. (1998) Calcium regulation of phototransduction in vertebrate rod outer segments. *J. Photochem. Photobiol.*, **44**, 1–20.

Rispoli, G., Martini, M., Rossi, M.L. & Mammano, F. (2001) Dynamics of intracellular calcium in hair cells isolated from the semicircular canal of the frog. *Cell Calcium*, **30**, 131–140.

Rispoli, G., Navangione, A. & Vellani, V. (1995) Transport of K by photoreceptor Na/Ca,K exchanger in isolated rods of lizard retina. *Biophys. J.*, **69**, 74–83.

Rispoli, G., Navangione, A. & Vellani, V. (1996) Turnover rate and number of Na: Ca,K exchange sites in retinal photoreceptors. *Ann. NY Acad. Sci.*, **779**, 346–356.

Rossi, M.L., Martini, M., Pelucchi, B. & Fesce, R. (1994) Quantal nature of synaptic transmission at the cytoneural junction in the frog labyrinth. *J. Physiol. (Lond.)*, **478**, 17–35.

Tucker, T. & Fettiplace, R. (1995) Confocal imaging of calcium microdomains and calcium extrusion in turtle hair cells. *Neuron*, **15**, 1323–1335.

Viappiani, C., Bacchi, A., Carcelli, M., Pelagatti, P. & Rogolino, D. (2002) Fast release of Ca^{2+} by two new photolabile chelators. *Biophys. J.*, **82**, 267a.

Yamoah, E.N., Lumpkin, E.A., Dumont, R.A., Smith, P.J., Hudspeth, A.J. & Gillespie, P.G. (1998) Plasma membrane Ca^{2+}-ATPase extrudes Ca^{2+} from hair cell stereocilia. *J. Neurosci.*, **18**, 610–624.